Rapid Quantitative Characterization of Protein Interactions by Composition Gradient Static Light Scattering

Keiichi Kameyama and Allen P. Minton
Laboratory of Biochemistry and Genetics, National Institute of Diabetes and Digestive and Kidney Diseases, National Institutes of Health, U.S. Department of Health and Human Services, Bethesda, Maryland

ABSTRACT Two new applications of the recently developed technique of composition gradient static light scattering (CG-SLS) are presented. 1), The method is demonstrated to be capable of detecting and quantitatively characterizing reversible association of chymotrypsin and bovine pancreatic trypsin inhibitor in a solution mixture and simultaneously occurring reversible self-association of chymotrypsin at low pH in the same mixture. The values of equilibrium constants for both self- and hetero-association may be determined with reasonable precision from the analysis of data obtained from a single experiment requiring $<$15 min and $<$1 mg of each protein. 2), Analysis of the results of a single CG-SLS experiment carried out on Ftsz, a protein that self-associates to form linear oligomers of indefinite size in the presence of guanosine diphosphate, yields the dependence of the equilibrium constant for monomer addition upon oligomer size.

INTRODUCTION

Quantitative characterization of reversible macromolecular associations in solution is an essential component of research aimed at understanding the function of these macromolecules in a biological system (1,2). We have recently introduced a light-scattering based method, called composition gradient static light scattering (CG-SLS), and demonstrated the capability of this method to rapidly detect and quantitatively characterize limited self-association equilibria in a solution containing a single protein component (3) and limited heteroassociation equilibria in a solution containing two protein components (4). The purpose of this article is to demonstrate two additional capabilities of this method:

1. The simultaneous detection and quantitative characterization of both self- and hetero-association equilibria in a solution containing two protein components.
2. The detection and characterization of indefinite self-association in a solution containing a single protein component.

MATERIALS AND METHODS

Materials

Chymotrypsin and bovine pancreatic trypsin inhibitor (BPTI) were obtained from Sigma (St. Louis, MO), dialyzed against phosphate buffer, 0.05 M Na Phosphate + 0.2 M NaCl, previously titrated to the indicated pH value, and used without further purification. FtsZ, prepared in a buffer containing 50 mM Tris-HCl + 50 mM KCl + 0.1 mM GDP + 5 mM $MgCl_2$, pH 7.5 (5), was a gift from Dr. Germán Rivas, CIB-CSIC. Protein concentrations were determined from the absorbance at 280 nm using the following standard values for absorbance in OD units/cm pathlength for a 1 g/l solution: chymotrypsin, 2.04 (6); bovine pancreatic trypsin inhibitor, 0.658 (7); and FtsZ, 0.345 (5). Refractive increments were determined as described in Attri and Minton (3), and found to be equal to 0.185 $\pm$ 0.003 ml/g at 20°C for all proteins utilized in this study. Immediately before light scattering measurement, solutions were prefiltered and centrifuged as described in Attri and Minton (3). Measurements of light scattering were carried out at 20°C.

Experimental procedures

Experiments are conducted utilizing the apparatus described in Attri and Minton (4), and depicted schematically in Fig. 1. The apparatus consists of a programmable dual-syringe pump (Model No. 541C, Hamilton, Reno, NV) configured to deliver a solution of time-varying composition—the composition gradient—to the flow cells of a light scattering detector (DAWN-EOS, Wyatt Technology, Santa Barbara, CA) and an UV-visible absorbance detector (Model No. SM5100, Milton Roy, Miami, FL). The two flow cells are connected in parallel to provide simultaneous measurements of scattering and absorbance of volume elements of solution with identical composition throughout the composition gradient.

Experiments on a single protein are performed as described in Attri and Minton (3). A solution of the protein is loaded into one solution reservoir, and buffer is loaded into the second. The composition gradient is obtained by incrementally increasing the flow rate from one syringe and simultaneously decreasing the flow rate from the second syringe to maintain a constant total flow rate. At user-specified intervals, the syringe pumps are halted to ensure equilibration of the mixture. In this fashion, a stepwise gradient of increasing or decreasing protein concentration is established.

Experiments on mixtures of proteins A and B are performed as described in Attri and Minton (4). A solution of A is loaded into one reservoir, and a solution of B is loaded into the second. By simultaneously increasing the flow rate from one syringe and decreasing the flow rate from the second syringe, a composition gradient is established in which the concentration of one protein increases and the second decreases, so that the mole fraction of one protein in the mixture gradually increases from 0 to 1, as the mole fraction of the second decreases from 1 to 0.

Raw data obtained from these two types of experiments were processed as described previously, and saved either as files of $\{w_{tot}, \langle R\rangle/K\}$ in the case of one-component experiments (3), or $\{f_A, \langle R\rangle/K\}$ in the case of two-component experiments (4), where w_{tot} denotes the total concentration of protein in units of g/l, $\langle R\rangle/K$ denotes the Rayleigh ratio, averaged from data obtained by multiple detectors, scaled to an optical constant K defined in Attri and Minton (3), and f_A denotes the fraction of the solution containing

Submitted September 12, 2005, and accepted for publication November 22, 2005.

Address reprint requests to Dr. Allen P. Minton, Bldg. 8, Rm. 226, National Institutes of Health, Bethesda, MD 20892-0830. Tel.: 301-496-3604; E-mail: minton@helix.nih.gov.

Keiichi Kameyama's permanent address is Dept. of Biomolecular Science, Faculty of Engineering, Gifu University, Yanagido 1-1, Gifu 501-1193 Japan.

0006-3495/06/03/2164/06 $2.00

doi: 10.1529/biophysj.105.074310

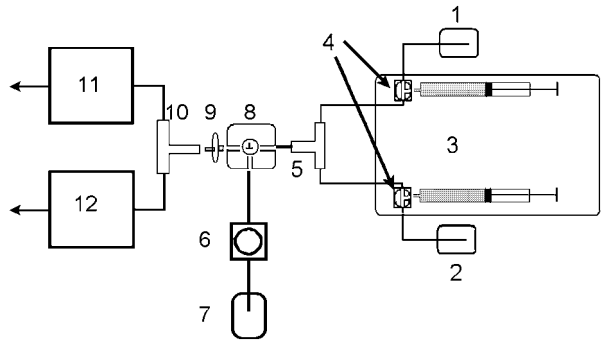

FIGURE 1 Schematic illustration of instrumentation used to perform composition gradient light scattering measurements: (*1–2*) Reservoirs for solutions *A* and *B*. (*3*) Programmable dual syringe pump. (*4*) Programmable valves for switching syringes between filling and delivery modes. (*5*) T-junction for mixing of input streams from the two syringes. (*6*) Peristaltic pump for delivery of buffer in reservoir (*7*). (*8*) Valve for switching apparatus input between peristaltic pump (*6*) and syringe pump (*3*). (*9*) Inline filter. (*10*) T-junction for splitting solution mixture into parallel streams for concurrent measurement in absorbance detector flow cell (*11*) and multi-angle light scattering detector flow cell (*12*). Figure reproduced from Attri and Minton (4).

component A in the two-component solution mixture. Raw data were acquired using ASTRA (V.4.7, Wyatt Technology), and exported as text files for subsequent processing and modeling in MatLab (Ver. 7.01, The MathWorks, Natick, MA). User-written MatLab scripts and functions used to perform calculations in this work are available upon request.

Modeling the composition dependence of the scaled Rayleigh ratio

In a solution containing a single protein component, absorbance data were converted to values of w_{tot} as described in Attri and Minton (3), and in a solution containing two protein components, absorbance data were converted to values of $w_{A,tot}$ and $w_{B,tot}$ as described in Attri and Minton (4). To calculate the value of R/K as a function of w_{tot} in a one-component experiment, or $w_{A,tot}$ and $w_{B,tot}$ in a two-component experiment, it is necessary to construct a model specifying the equilibrium concentrations of all macromolecular solute species present in detectable quantity as a function of the total w/v concentration of each protein component. The general procedure for doing so is presented in Attri and Minton (4). Here we present two specific models that were applied to the analysis of the data presented here.

Model 1: chymotrypsin (A) + bovine pancreatic trypsin inhibitor (B)

On the basis of known association properties of these two proteins (8,9), the following species are postulated: monomeric A, monomeric B, a heterodimer (AB), and a homodimer (AA). In accordance with notation introduced in Attri and Minton (4), wherein a property of species A_iB_j is indicated by the subscript $\{ij\}$, we define the following equilibrium constants for hetero-association of A and B, and for self-association of A, respectively:

$$K_{11} = \frac{c_{11}}{c_{10}c_{01}}, \tag{1}$$

$$K_{20} = \frac{c_{20}}{c_{10}^2}. \tag{2}$$

The equations of conservation of mass are then

$$c_{A,tot} = \frac{w_{A,tot}}{M_A} = c_{10} + 2c_{20} + c_{11} = c_{10} + 2K_{20}c_{10}^2 + K_{11}c_{10}c_{01}, \tag{3}$$

$$c_{B,tot} = \frac{w_{B,tot}}{M_B} = c_{01} + c_{11} = c_{01} + K_{11}c_{10}c_{01}. \tag{4}$$

Given the experimentally determined values of $w_{A,tot}$, $w_{B,tot}$, and test values of M_A, M_B, K_{11}, and K_{20}, Eqs. 3 and 4 may be solved numerically for the values of c_{10} and c_{01}, and c_{11} and c_{20} are then obtained via Eqs. 1 and 2. The scaled Rayleigh ratio is then calculated according to Attri and Minton (4):

$$R/K = M_{10}^2c_{10} + M_{01}^2c_{01} + M_{11}^2c_{11} + M_{20}^2c_{20}. \tag{5}$$

Model 2: indefinite self-association of FtsZ

In the presence of GDP and Mg, FtsZ has been shown to undergo indefinite self-association to form linear oligomers (5). Accordingly, the following set of equilibrium constants for stepwise addition of monomer to oligomer are defined for $i \geq 2$,

$$K_i \equiv \frac{c_i}{c_{i-1}c_1}, \tag{6}$$

where c_i denotes the molar concentration of i-mer, and $K_1 \equiv 1$. The condition of conservation of mass is expressed as

$$c_{tot} = w_{tot}/M_1 = \sum_i ic_i = \sum_i iQ_ic_1^i, \tag{7}$$

where M_1 is the molar mass of monomeric protein, and

$$Q_i = \prod_{j=1}^{i} K_i. \tag{8}$$

According to the theory of isoenthalpic linear indefinite self-association of identical subunits (10), the value of K_i should gradually decrease with increasing oligomer size and approach a constant value, denoted K_∞, in the limit of large oligomer size. Therefore we define a unitless scaling factor $F_i \equiv K_i/K_\infty$ for $i > 1$, such that $F_2 > 1$ and $F_i \rightarrow 1$ as $i \rightarrow \infty$, and $F_1 \equiv 1$. Then

$$Q_i = K_\infty^{i-1}Z_i, \tag{9}$$

where

$$Z_i = \prod_{j=1}^{i} F_j.$$

We now define the unitless protein concentrations $c_{tot}^* \equiv K_\infty c_{tot}$ and $c_1^* \equiv K_\infty c_1$. It follows then from Eqs. 7–9 that

$$c_{tot}^* = \sum_i iZ_ic_1^{*i}. \tag{10}$$

Given an experimental value of w_{tot} and test values of M_1, K_∞, and the Z_i, Eq. 10 may be solved numerically for the value of c_1*. Then from Eq. 9,

$$c_i = \frac{Z_i}{K_\infty}c_1^{*i}, \tag{11}$$

and the scaled Rayleigh ratio may be calculated according to

$$R/K = \sum M_i^2c_i = \frac{M_1^2}{K_\infty}\sum i^2Z_ic_1^{*i}. \tag{12}$$

It is evident that the above model, which contains an arbitrary number of independently variable F_i or the equivalent Z_i, must be simplified. This is

done by specifying a simple empirical functional dependence of F_i upon i obeying the conditions set out in the above definition of F_i. It was shown previously that so long as the final calculated dependence of experimental signal upon total protein concentration is in agreement with experiment, the underlying distribution of species is independent of the precise form of the empirical function employed (5). We therefore select one of the empirical forms utilized by Rivas et al. (5) for $i > 1$:

$$F_i = 1 + \frac{J - 1}{(i - 1)^{\alpha}}. \quad (13)$$

Thus, specification of the test values of the empirical parameters J and α together with K_∞ and M_1 permits the calculation of R/K as a function of w_{tot}. (In the numerical calculation, sums over species indicated above were evaluated up to $i = 100$. It was verified that all series converged well before this limit.)

RESULTS AND DISCUSSION

Chymotrypsin (A) + bovine pancreatic trypsin inhibitor (B)

Experiments were carried out over a range of pH values, in solutions prepared as described in Materials and Methods. The dependence of $\langle R \rangle / K$ on f_A obtained at three pH values is plotted in Fig. 2. Initially, unsuccessful attempts were made to analyze the composition gradient data in the context of a simple 1-1 hetero-association model, but it was soon realized that derived values of the molar mass of chymotrypsin were dependent upon pH and unrealistically high at low pH values. Reference to the literature then revealed that chymotrypsin is known to dimerize significantly under acid conditions (8,11). (This is a graphic example of how the results obtained using the present technique can rapidly guide the investigator to the correct choice of association model.) Subsequently, the data were analyzed in the context of the model described by Eqs. 1–5 above. To obtain the maximum amount of information about this two-component system, three separate experiments were carried out on solutions prepared at each of several different pH values. Dilution (one-component) experiments of the type described in Attri and Minton (3) were carried out on solutions of each of the two proteins, and then the composition gradient (two-component) experiment described in Attri and Minton (4) was carried out on a time-varying mixture of the two proteins. Two alternate modeling procedures were then carried out. In the first procedure (single-scan modeling), only the results of the two-component experiment were fit by the model equations. The best fit of the hetero- plus self-association model obtained in this manner at three pH values is plotted together with the data in Fig. 2. Using the values of best-fit parameters, the concentrations of individual species and the contributions of individual species to the total scattering may be calculated, and these are plotted in Fig. 3. In the second procedure (global modeling), a compound model was constructed to simultaneously fit the results of the two-component experiment together with the results from either one or two one-component experiments, to simultaneously evaluate best-fit values of M_A, M_B, log K_{20}, and log K_{11}. Best-fit values and uncertainties of equilibrium association constants determined by single scan and global modeling are presented in Table 1. Best-fit values of equilibrium constants for hetero- and self-association are plotted as functions of pH in Fig. 4, *a* and *b*, respectively.

Although estimates of the association constants obtained by different treatments of the present data are reasonably self-consistent, values of log K_{11} obtained in this study are systematically 5–10-fold lower at all pH values than those reported earlier by Vincent and Lazdunski (9), although the pH dependence is approximately the same. There are at least two possible explanations for the discrepancy:

1. The difference may be due to the difference in buffers employed in the two studies. The equilibrium constants presented by Vincent and Lazdunski (9) were calculated as the ratio of directly measured association and dissociation rate constants, and dissociation rates were measured in a buffer containing 50 mM $CaCl_2$ in addition to NaCl. Substitution of Ca^{2+} for Na^+ has been found to significantly enhance noncovalent associations of a variety of other proteins, including the self-association of chymotrypsin (see, for example, (11–14)), and we feel that this is likely to be the case for associations between chymotrypsin and BPTI as well.
2. Discrepancy between the actual equilibrium constant and the apparent equilibrium constant calculated via the ratio of association and dissociation rate constants may arise if the complex AB exists as a mixture of two isomers in rapid equilibrium, only one of which undergoes dissociation. The actual and apparent equilibrium constants will then differ by a constant reflecting the fraction of AB existing as the dissociating isomer at equilibrium.

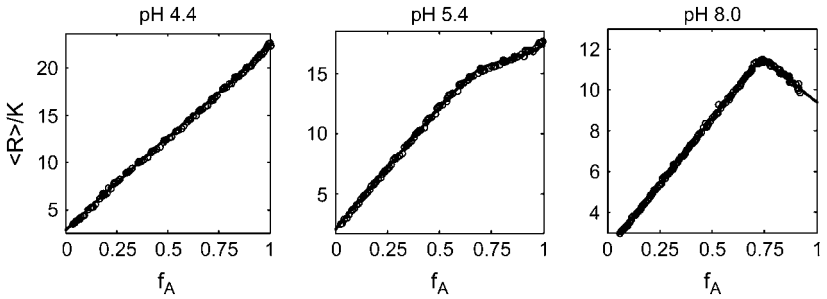

FIGURE 2 $\langle R \rangle / K$ plotted as a function of f_A for a composition gradient of chymotrypsin (A) and bovine pancreatic trypsin inhibitor at three pH values. The curves represent the dependence calculated with the equilibrium model described by Eqs. 1–5 using best-fit parameter values listed in Table 1, obtained via global modeling as described in the text.

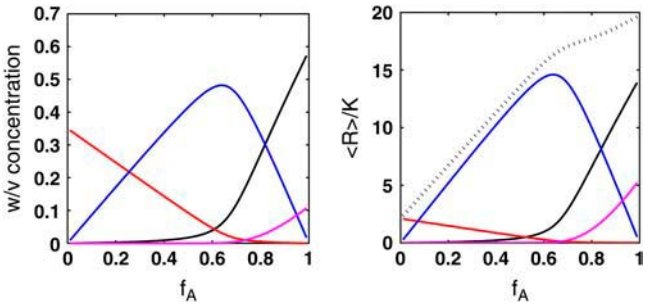

FIGURE 3 Contributions of individual species to the composition gradient scattering profile, calculated using parameters obtained from the best fit of the equilibrium model described by Eqs. 1–5 to the data obtained at pH 5.4 (*center panel* of Fig. 1; see also Table 1). (*Left*) Calculated concentrations of individual species. (*Right*) Calculated concentrations of individual species (*solid lines*) to the total scattering profile (*dotted line*). Individual species are indicated by colors as follows: *A*, black; *B*, red; *AB*, blue; and A_2, magenta.

We had hoped that global modeling of multiple experiments would significantly increase the precision of results obtained from analysis of the combined data, but the results presented in Table 1 do not fulfill this expectation. We believe that this is partly due to the fact that the individual one-component experiments and the two-component composition gradient experiments were carried out at different times, using different protein solutions. In addition to possible differences between the solutions used in the individual experiments, there exists also the possibility of slight changes in instrumental sensitivity. (The light scattering detector is recalibrated periodically—typically once every two months—but not before each experiment.) A protocol for rapid sequential performance of the combined experiments using the same solutions is under development.

TABLE 1 Best-fit parameter values obtained from modeling composition gradients of chymotrypsin (A) and BPTI (B)

pH	log K_{20}	log K_{11}	M_A /10^3	M_B /10^3
4.4	*4.0 (±0.25)*	*4.5 (±0.45)*	*27.0 (±0.35)*	*5.3 (±0.35)*
	4.3 (±0.2)	5.0 (−0.4, + 0.6)	24.7 (±0.15)	5.6 (±0.3)
4.9	*3.8 (− ∞, + 0.5)*	*5.4 (±1.3)*	*25.4 (±0.25)*	*5.4 (±0.7)*
	4.1 (±0.15)	5.85 (−0.5, + 0.6)	23.9 (±0.1)	5.7 (±0.2)
5.4	*3.7 (±0.2)*	*6.2 (−0.6, + 1.0)*	*23.6 (±0.1)*	*6.1 (±0.25)*
	3.5 (±0.2)	6.0 (±0.5)	24.3 (±0.8)	5.9 (±0.2)
6.7	*3.2 (−0.7, + 0.2)*	*6.8 (−0.7, + ∞)*	*22.9 (±0.1)*	*5.9 (±0.3)*
	2.8 (− ∞, + 0.3)	6.4 (−0.4, + 1.0)	23.5 (±0.1)	5.7 (±0.2)
7.3	*3.2 (±0.2)*	*7.0 (−0.6, + ∞)*	*23.1 (±0.05)*	*5.9 (±0.2)*
	3.0 (−0.5, + 0.3)	7.1 (−0.7, + ∞)	23.2 (±0.5)	5.9 (±0.35)
8.0	*3.1 (− ∞, + 0.4)*	*7.2 (−0.9, + ∞)*	*21.2 (±0.05)*	*5.2 (±0.2)*
	2.7 (− ∞, + 0.3)	6.8 (−0.5, + ∞)	21.4 (±0.3)	5.2 (±0.1)

Values in italics were obtained by modeling the results of a single composition gradient experiment. Values in Roman font were obtained by modeling the results of the composition gradient experiment together with the results of a dilution experiment carried out on a solution of chymotrypsin alone and, in some cases, with the results of a dilution experiment carried out on a solution of BPTI alone.

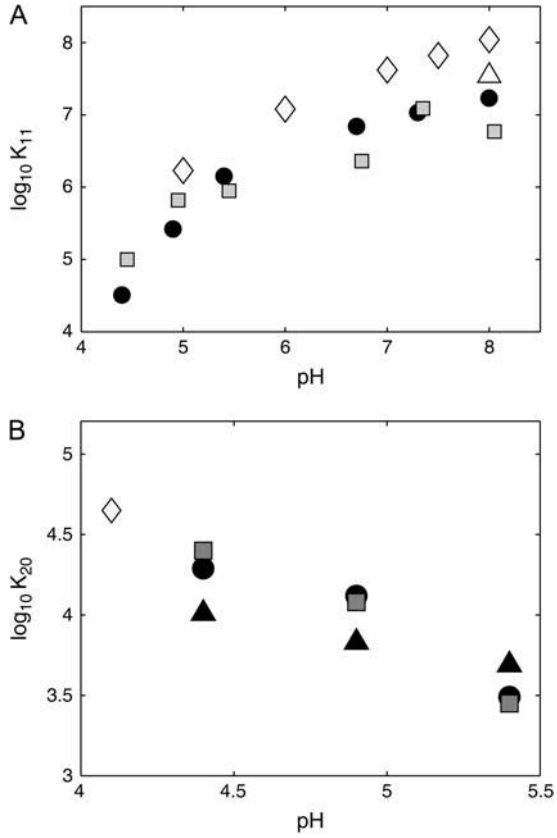

FIGURE 4 Best-fit values of equilibrium association constants characterizing hetero-association of chymotrypsin and BPTI (*A*) and self-association of chymotrypsin (*B*), plotted as a function of pH. (*A*) Circles, values obtained by modeling a single composition gradient experiment. Squares, values obtained by global modeling of a composition gradient together with one or two dilution experiments conducted on individual proteins. Diamonds, values reported by Vincent and Lazdunski (9), calculated from ratio of measured association and measured rate constants. Triangle, value reported by Rigbi, as quoted in Vincent and Lazdunski (9). (*B*) Triangles, values obtained from modeling a single composition gradient experiment. Squares, values obtained from modeling a single dilution experiment conducted on pure chymotrypsin. Circles, values obtained from global modeling of composition gradient and dilution experiments. Diamond, value reported by Aune and Timasheff (8).

FtsZ

Replicate dilution experiments were carried out as described previously (3) on the protein solution described in Materials and Methods. The experimentally measured dependence of $\langle R\rangle/K$ upon w_{tot} is plotted in Fig. 5. The model described by Eqs. 6–13 was fit to the experimental data, fixing the value of M_1 at 40,500 (5). A broad variety of combinations of the parameters K_∞, J, and α were found capable of fitting the data to within experimental precision, indicating that these parameters are highly correlated, and hence may not be determined individually. One of the (identical) calculated best-fits is plotted in Fig. 5 together with the data. One can calculate stepwise equilibrium constants and standard free energies of stepwise association as functions of oligomer size using each

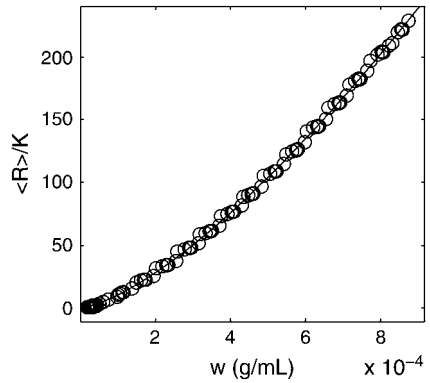

FIGURE 5 Concentration-dependent scattering of FtsZ as a function of total protein concentration. (*Points*, experimental data; *curve*, dependence calculated from inverse-decay model, using any of a several sets of correlated parameter values leading to identical fits of the data.)

of the sets of model parameters that fits the data to within experimental precision. In Fig. 6, calculated values are plotted for a number of such parameter sets, and it is evident that stepwise equilibrium constants and free energies of monomer association so calculated are uniquely determined to high precision, independent of the particular parameter set, so long as that parameter set is capable of fitting the experimental data to within experimental precision.

Also plotted in Fig. 6 are comparable values obtained from analysis of sedimentation equilibrium experiments conducted on FtsZ under nominally identical experimental conditions (5). In view of the fact that the two sets of measurements were conducted more than five years apart by different investigators using entirely different techniques, the agreement between the stepwise free energies obtained by the two methods (generally better than $\sim$0.1 *RT*) is particularly impressive.

SUMMARY

In this work, the technique of composition gradient static light scattering, developed recently in our laboratory (3,4) is shown to be capable of characterizing interacting systems more complex than those treated in previous publications. In the first example, the technique successfully detected and characterized pH-dependent reversible heteroassociation of chymotrypsin and bovine pancreatic trypsin inhibitor, and self-association of chymotrypsin taking place in the same solution under acidic conditions. We are unaware of any previous report of detection, much less quantitative characterization, of both self- and hetero-association equilibria in the same solution by any analytical technique. In the second example, the technique was used to characterize the indefinite linear self-association of a protein (FtsZ-GDP) and to precisely determine standard-state free energies of successive addition of monomer to growing oligomers. The results are in excellent agreement with those obtained earlier via sedimentation equilibrium. We emphasize that the data shown in Fig. 5 and analyzed in Fig. 6, were obtained in a single experiment of $<$15 min duration, whereas the equivalent information obtained via sedimentation equilibrium required experiments of several days duration (G. Rivas, personal communication, 2005).

The success of CG-SLS in resolving association equilibria may be attributed to the high information content of the composition-dependent scattering profile, which becomes evident when the contributions of individual species to the total scattering profile are quantified, as exemplified by the right-hand panel of Fig. 3. The dependence of equilibrium concentrations of individual macrosolute species—and hence the total scattering profile—upon overall solution composition as it varies along the f_A coordinate is extremely sensitive to differences between alternative reaction schemes and small changes in equilibrium constants within a particular scheme.

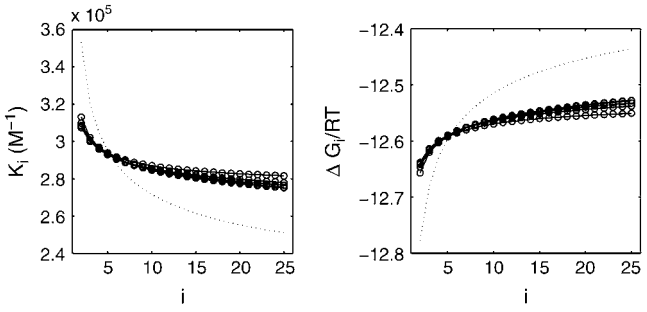

FIGURE 6 K_i (*A*) and G_i (*B*) for addition of monomer to form *i*-mer, plotted as a value of *i*. Symbols were calculated using each of the sets of correlated parameter values consistent with the experimentally observed dependence of $\langle R\rangle/K$ on w_{tot} depicted in Fig. 5. The curve was calculated using the parameters obtained by modeling sedimentation equilibrium data as described in Rivas et al. (5).

We thank Dr. Germán Rivas (Center for Biological Research, Madrid) for a gift of FtsZ, Dr. Jose Manuel González (Center for Biological Research, Madrid) for assistance with preliminary experiments on FtsZ, and for Dr. Peter McPhie, National Institute of Diabetes and Digestive and Kidney Diseases (NIDDK), for critical reading of manuscript drafts.

This research was supported by the Intramural Research Program of NIDDK, National Institutes of Health, and in part by the appointment of K. Kameyama to the NIDDK Research Participation Program, administered by the Oak Ridge Institute of Science and Education.

REFERENCES

1. Phizicky, E. M., and S. Fields. 1995. Protein-protein interactions: methods for detection and analysis. *Microbiol. Rev.* 59:94–123.
2. Srere, P. A., editor. 1999. Special Issue: Heterologous protein-protein interactions. *Methods.* 19:191–349.
3. Attri, A. K., and A. P. Minton. 2005. New methods for measuring macromolecular interactions in solution via static light scattering: basic methodology and application to nonassociating and self-associating proteins. *Anal. Biochem.* 337:103–110.
4. Attri, A. K., and A. P. Minton. 2005. Composition gradient static light scattering (CG-SLS): a new technique for rapid detection and quantitative characterization of reversible macromolecular hetero-associations in solution. *Anal. Biochem.* 346:132–138.
5. Rivas, G., A. Lopez, J. Mingorance, M. J. Ferrándiz, S. Zorrilla, A. P. Minton, M. Vicente, and J. M. Andreu. 2000. Magnesium-induced

linear self-association of the FtsZ bacterial cell division protein monomer. *J. Biol. Chem.* 275:11740–11749.

6. Morimoto, K., and G. Kegeles. 1967. Dimerization and activity of chymotrypsin at pH 4. *Biochemistry.* 6:3007–3010.
7. Kazal, L. A., D. S. Spicer, and R. A. Brahinsky. 1948. Isolation of a crystalline trypsin inhibitor—anticoagulant protein from pancreas. *J. Am. Chem. Soc.* 70:3034–3040.
8. Aune, K. C., and S. N. Timasheff. 1971. Dimerization of α-chymotrypsin. I. pH dependence in the acid region. *Biochemistry.* 10:1609–1617.
9. Vincent, J.-P., and M. Lazdunski. 1973. The interaction between α-chymotrypsin and pancreatic trypsin inhibitor. *Eur. J. Biochem.* 38: 365–372.
10. Chatelier, R. C. 1987. Indefinite isoenthalpic self-association of solute molecules. *Biophys. Chem.* 28:121–128.
11. Aune, K. C., L. C. Goldsmith, and S. N. Timasheff. 1971. Dimerization of α-chymotrypsin. II. Ionic strength and temperature dependence. *Biochemistry.* 10:1617–1622.
12. Rivas, G., K. C. Ingham, and A. P. Minton. 1994. Ca^{2+} linked association of human complement C1s and C1r. *Biochemistry.* 33:2341–2348.
13. Yu, X. C., and W. Margolin. 1997. Ca-mediated GTP-dependent dynamic assembly of bacterial cell division protein FtsZ into asters and polymer networks in vitro. *EMBO J.* 16:5455–5463.
14. Rivas, G., J. A. Fernández, and A. P. Minton. 1999. Direct observation of the self-association of dilute proteins in the presence of inert macromolecules at high concentration via tracer sedimentation equilibrium: theory, experiment, and biological significance. *Biochemistry.* 38:9379–9388.